Computers and Geotechnics 67 (2015) 229–238

Contents lists available at ScienceDirect

Computers and Geotechnics

journal homepage: www.elsevier.com/locate/compgeo

Research Paper

Influence of embedment, self-weight and anisotropy on bearing capacity reliability using the random finite element method

J.M. Pieczyńska-Kozłowska [a,*], W. Puła [a], D.V. Griffiths [b], G.A. Fenton [c]

[a] Department of Civil Engineering, Wrocław University of Technology, Wybrzeże Wyspiańskiego 27, 50-370 Wrocław, Poland
[b] Department of Civil & Environmental Engineering, Colorado School of Mines, 1500 Illinois Street, Golden, CO 80401, USA
[c] Dalhousie University, 1360 Barrington Street, PO Box 15000, Halifax, NS B3H 4R2, Canada

ARTICLE INFO

Article history:
Received 24 July 2014
Received in revised form 30 January 2015
Accepted 22 February 2015
Available online 3 April 2015

Keywords:
Random finite element method
Bearing capacity
Strip foundation
Anisotropic random field

ABSTRACT

The paper expands on previous work by the authors on bearing capacity of random $c' - \phi'$ soils using the random finite element method. The refinements in the present work include the influence of embedment, soil self-weight and anisotropy which were not considered previously. The study focuses on a grey-blue clay from Taranto in Italy, for which stochastic strength parameters were well documented. Results show that the influences of embedment, self-weight and anisotropy can be significant and lead to more realistic estimates of bearing capacity reliability. Finally a probability distribution of the bearing capacity was estimated and used to calibrate safety factors for reliability purposes.

1. Introduction

An increasing number of studies in the field of geotechnical engineering are considering the random character of subsoil when analysing the bearing capacity of a shallow foundation. This issue is important because it allows for the optimisation of structures that interact with soil, which are often a substantial part of the design and construction processes. The basic approach is to model the random variability of soil properties. Several papers on this subject were published in the 1960s and early 1970s, including the pioneering works of Lumb [21,22] and Schultze [29]. With the development of numerical methods and the increasing computational ability of computers, techniques for including the spatial variability of soil have been developed, leading to the modelling of soil parameters via random fields. The concepts of random functions and random fields appeared in papers by Lumb [23] and Alonso and Krizek [3]. In particular, the work of Vanmarcke [31–33] was of great importance to subsequent research. Applications of random fields in the modelling of soil parameters grew significantly following the work of Fenton and Vanmarcke [10], who developed methods of generating random fields with the use of the local average subdivision (LAS). Similar concepts have appeared in the modelling of geological deposits, especially in the work of Krige [19,20] and Zubrzycki [34]. It was only after random field concepts were combined with advanced finite element analysis [16] that meaningful practical geotechnical applications became feasible.

Griffiths and Fenton [15], Fenton and Griffiths [11] and Fenton et al. [14] studied the bearing capacity of a shallow foundation on soil with random characteristics. The analyses were performed using the random finite element method (RFEM), whose algorithms are a combination of random field theory, the classical finite element method (FEM) and Monte Carlo simulations (e.g., Fenton and Griffiths [13]). A special feature of this algorithm is that it uses multiple repetitions of calculations for different realisations of the random field. Thus, both the expected value of the random resistance from the realisation set and the probability distribution can be estimated with the use of Monte Carlo simulations and the resulting large number of realisations.

In recent years there have been a few modelling studies combining random fields with FEM for bearing capacity evaluations. In the paper by Kasama and Whittle [18] the bearing capacity of undrained soil was investigated using numerical limit analysis. In this study the undrained shear strength was modelled as an isotropic random field. The paper by Rahman and Nguyen [27] also considered undrained bearing capacity but expanded the analyses to include anisotropic random field modelled by Local Average Subdivision Method. Cassidy et al. [6] considered combined loading of strip footings subjected to vertical, horizontal and moment

* Corresponding author.
E-mail addresses: joanna.pieczynska-kozlowska@pwr.edu.pl (J.M. Pieczyńska-Kozłowska), wojciech.pula@pwr.edu.pl (W. Puła), d.v.griffiths@mines.edu (D.V. Griffiths), gordon.fenton@dal.ca (G.A. Fenton).

http://dx.doi.org/10.1016/j.compgeo.2015.02.013
0266-352X/

Nomenclature

c	cohesion
ϕ	friction angle
ν	Poisson ratio
E	Young's modulus
γ	soil unit weight
π	PI
B	footing width
D	footing high of embankment
$q_f = q_{ult}$	ultimate bearing capacity
q_{FEM}	bearing capacity value computed by finite element method
q_d	bearing capacity design value
N_c	bearing capacity factor – cohesion
N_γ	bearing capacity factor – unit weight
N_q	bearing capacity factor – overburden pressure
p_f	probability of failure
β	reliability index
Φ	cumulative distribution function of the standard distribution
x_i	single realisation of random variable x
$f(x)$	probability density function
$E[X]$	expected value
Var[X]	variance
ρ	correlation function
τ	separation vector absolute distance between points in field
γ^{VAR}	Variance reduction function
μ_{lnx}	mean value in underlying normal distribution
μ_c	mean value of cohesion
μ_ϕ	mean value of friction angle
μ_x	mean value in lognormal distribution
μ_{qf}	mean value of bearing capacity
σ_x	standard deviation in lognormal distribution
σ_{lnx}	standard deviation in underlying normal distribution
σ_c	standard deviation of cohesion
σ_ϕ	standard deviation of friction angle
σ_{qf}	standard deviation of bearing capacity
COVc	coefficient of variation of cohesion
COVϕ	coefficient of variation of friction angle
COVq_f	coefficient of variation of bearing capacity
θ	fluctuation scale, correlation length
θ_c	fluctuation scale of cohesion
θ_ϕ	fluctuation scale of friction angle
θ_x	horizontal fluctuation scale
θ_y	vertical fluctuation scale
θ/B	fluctuation scale normalised on footing width
G_{lnc}	Gaussian random field of cohesion
G_ϕ	Gaussian random field of friction angle
FS	factor safety

loads. It is worth mentioning new simulation approaches recently proposed by Ahmed and Soubra [1] and by Al-Bittar and Soubra [2]. Fenton and Griffiths [11] analysed the bearing capacity of a surface footings on $c' - \phi'$ soils, i.e., soils with no footing embedment. In that study, the soil unit weight was ignored and the random fields of cohesion and the internal friction angle were assumed to be isotropic, i.e., the spatial correlation was the same in both the vertical and horizontal directions.

This article is a supplement to and continuation of the aforementioned work. The algorithm used by Fenton and Griffiths [11] was expanded to consider foundation embedment and soil unit weight. In addition, the influence of anisotropic random fields and the cross-correlation between soil parameters was investigated.

2. Assumptions used in the computations

The traditional computational approach of estimating the bearing capacity under drained conditions presupposes the designation of the bearing capacity with the use of the Terzaghi equation [30], which is based on the mechanism described by Prandtl [25]:

$$q_f = c' N_c + q N_q + \frac{1}{2}\gamma B N_\gamma \tag{1}$$

where q_f is the bearing capacity, c' is the cohesion, q is the overburden pressure, γ is the soil unit weight, B is the footing width, and N_c, N_q and N_γ are the bearing capacity factors, which depend on the internal friction angle, ϕ'. The study by Fenton and Griffiths [11], using the RFEM, only considered the component of Eq. (1) associated with the cohesion, i.e.,

$$q_f = c' N_c \tag{2}$$

in which the bearing capacity factor, N_c, is given by Ref. [25]:

$$N_c = \frac{\exp(\pi \tan\phi') \tan^2\left(\frac{\pi}{4} + \frac{\phi'}{2}\right) - 1}{\tan\phi'} \tag{3}$$

The current study includes all elements of Eq. (1) while also considering the influences of different effects of random soil resistance. The computational scheme of the study is summarised in Fig. 1.

Soil parameters were modelled as random fields characterised by probability distributions and a specified correlation structure. The soil analysed was Taranto Blue Clay, whose properties have been described by Cafaro et al. [4], Cafaro and Cherubini [5], Cherubini [8] and Cherubini et al. [9]. The statistical data were obtained using in situ tests, including CPT penetration tests.

Each test result is described using a trend function with the parameters corresponding to the mean value and residual variance of the parameter around the trend. The results are presented in Table 1.

The fluctuations of these values were then modelled using random fields with a zero mean and unit standard deviation. The correlation structure was isotropic and characterised by the vertical values of the fluctuation scale [31], which was measured by Cafaro and Cherubini [5]. Weak (or wide-sense) stationarity of

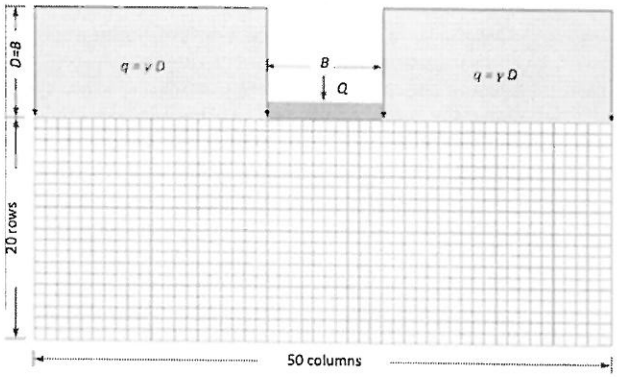

Fig. 1. Computational scheme used in the analysis.

Table 1
Trend and scale of fluctuations from CPT tests [5].

Borehole	Trend	Vertical scale of fluctuation θ_y (m)
Upper clay		
1	$y = 54.671x^2 - 21.21x + 5301$	0.195
2	$y = 12.44x^2 + 113.06x + 2950$	0.401
3	$y = 40.713x^2 - 439.7x + 5601$	0.207
4	$y = 73.690x^2 - 172.2x + 9753$	0.401
5	$y = 11.027x^2 + 212.3x + 2541$	0.436
Lower clay		
1	$y = 149.11x + 4732$	0.536
2	$y = 319.58x + 1722$	0.287
3	$y = 201.29x + 3700$	0.720
4	$y = 201.14x + 4036$	0.269
5	$y = 203.34x + 3699$	0.185

y denotes the cone resistance (kPa), and x is the depth (m).

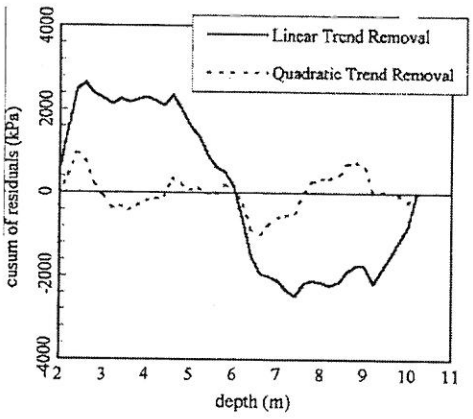

Fig. 2. CUSUM test for CPT testing of the upper layer in borehole 1 (c.f. Table 1); graph showing the residual parts remaining after removal of the linear and quadratic trends [5].

this field was verified by Cafaro et al. [4] via the CUSUM test [24]. An example is shown in Fig. 2.

To determine the scale of fluctuation, a method of aligning the theoretical correlation coefficient to the empirical one, as described by Vanmarcke [31], was applied. The vertical variability of the Taranto Blue Clay was determined by analysing the parameter variability over the sampled depth; it was further characterised by a scale of vertical fluctuations (see Table 1). Unfortunately, there was no analysis of the scale of horizontal fluctuations (θ_x) in the framework described by Cafaro et al. [5]. Soil property values of the Taranto Blue Clay strength parameters are presented in Table 2.

In the present study, a lognormal random field was applied for the cohesion to ensure non-negative values of x. The probability density function of a lognormal distribution is given by the following equation:

$$f(x) = \begin{cases} \frac{1}{x\sigma_{\ln x}\sqrt{2\pi}} \exp\left\{-\frac{1}{2}\left(\frac{\ln x - \mu_{\ln x}}{\sigma_{\ln x}}\right)^2\right\} & \text{if } x > 0 \\ 0 & \text{if } x \leqslant 0 \end{cases} \tag{4}$$

where $\mu_{\ln x}$ and $\sigma_{\ln x}$ are the underlying normal distribution parameters. The relationships between these parameters and the mean and variance of the lognormal distribution (μ_x, σ^2_x) are given as follows:

$$\mu_x = E[X] = \exp\left(\mu_{\ln x} + \frac{1}{2}\sigma^2_{\ln x}\right) \tag{5}$$

$$\sigma^2_x = \mathrm{Var}[X] = \mu^2_x(\exp(\sigma^2_{\ln x}) - 1) \tag{6}$$

Table 2
Characteristics of variable mechanical properties of the Taranto Blue Clay.

	Mean value μ_x	Standard deviation σ_x
Cohesion (c)	36 kPa	20 kPa
Friction angle (ϕ)	20°	4.8°
Self-weight (γ)	19 kN/m^3	Deterministic
Young's modulus (E)	36,000 kPa	Deterministic
Poisson ratio (ν)	0.29	Deterministic

The mean value (μ_x) and standard deviation (σ_x) were assigned the values shown in Table 2. In the case of the random field, which characterises the friction angle, a bounded distribution centred on the interval $[a, b]$ with the following probability density function was assumed, as proposed by Fenton and Griffiths [11]:

$$f(x) = \begin{cases} \frac{\sqrt{\pi}(b-a)}{\sqrt{2}s(x-a)(b-x)} \exp\left\{-\frac{1}{2s^2}\left[\pi \ln\left(\frac{x-a}{b-x}\right) - m\right]^2\right\} & \text{if } x \in (a,b) \\ 0 & \text{if } x \notin (a,b) \end{cases} \tag{7}$$

This distribution corresponds well with the bounded interval of the friction angle variability; the distribution depends on four parameters, the minimum ($a = \phi_{\min}$) and maximum ($b = \phi_{\max}$) values of the friction angle and two additional parameters, s and m. The parameter s affects the shape of the density function (and indirectly affects the standard deviation), and the parameter m affects the position of the mean value. In the case of $m = 0$, the mean value is in the middle of the interval $[\phi_{\min}, \phi_{\max}]$, and the standard deviation in the bounded distribution can only be approximated using the first-order Taylor expansion:

$$\sigma_x \approx \frac{1}{2}(b-a)\frac{2s}{\pi(e^{2\mu_x} - e^{-2\mu_x} + 2)} \tag{8}$$

Using the values in Table 2, the minimal value is set to $\phi_{\min} = 5°$, and the maximum value to $\phi_{\max} = 35°$, with $s = 2.27$ and $m = 0$.

The random fields for the mechanical properties of the soil were generated using local average subdivision (LAS) [10]. LAS yields a normal distribution; therefore, data must be transformed if non-normal distributions are required, as in this case (cohesion is log-normal and friction is angle-bounded). In the case of cohesion, the mean value and standard deviation of the underlying normal distribution ($\ln c$) are given by Eqs. (9) and (10), respectively.

$$\mu_{\ln c} = \ln \mu_c - \frac{1}{2}\sigma^2_{\ln c} \tag{9}$$

$$\sigma^2_{\ln c} = \ln\left(1 + \frac{\sigma^2_c}{\mu^2_c}\right) \tag{10}$$

The correlation structures of the underlying Gaussian random field, $G_{\ln c}(x)$, were determined using the Markov correlation coefficient, ρ:

$$\rho = \exp\left\{-\sqrt{\left(\frac{2\tau_2}{\theta_x}\right)^2 + \left(\frac{2\tau_1}{\theta_y}\right)^2}\right\} \tag{11}$$

where $\tau_1 = y_2 - y_1$ and $\tau_2 = x_2 - x_1$ define the absolute distance between the two points in 2D space and θ_x and θ_y are the values of the horizontal and vertical fluctuation scales, respectively. In the present study, the vertical fluctuation scale was based on results provided in Table 1. Therefore, four different value were considered: $\theta_y = 0.2$ m, $\theta_y = 0.5$ m, $\theta_y = 0.7$ m, and $\theta_y = 1.0$ m. The assumptions concerning the horizontal fluctuation scale, θ_x, are specified in Section 3.2. To generate fields, it is necessary to determine the respective scales of fluctuation. Theoretically, scales can be different for the cohesion (θ_c) and internal friction angle (θ_ϕ) fields, however

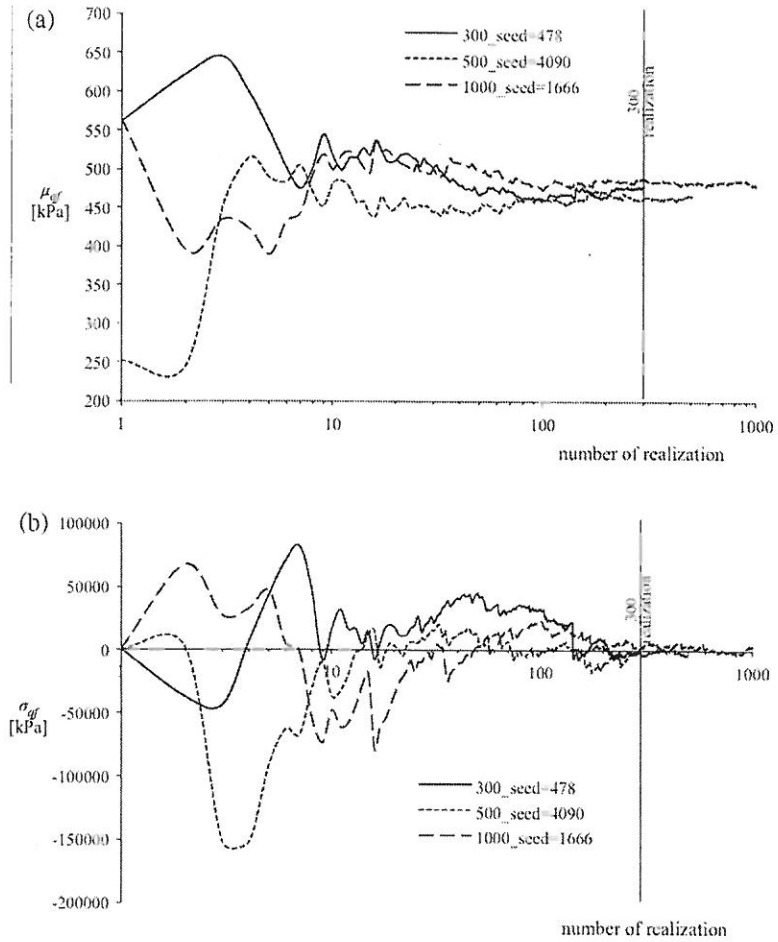

Fig. 3. Convergence speed of the random value of the bearing capacity: (a) mean value of the bearing capacity versus sample size; (b) standard deviation of the bearing capacity versus sample size.

within this study it has been assumed that fluctuations scales are the same for both strength parameters ($\theta_c = \theta_\phi$). This seems a reasonable assumption based on limited information (especially relating to spatial correlation lengths), but more importantly soil depositional processes. If the stiffness and strength are positively correlated in a soil, it seems reasonable that the spatial correlation trends for both parameters will be similar. Given the lack of good quality data on the spatial correlation properties of soil, the correlation lengths of the lognormal and normal fields are assumed to be sufficiently similar for the purposes of the parametric studies presented in this paper. Inclusion of the mathematical relationships between the correlations is beyond the scope of the present work, however the interested reader is referred to Fenton and Griffiths [12] for further discussion.

Moreover, it was assumed that the cohesion random field and internal friction angle random field were mutually stochastically independent. This assumption might be controversial because earlier papers reported a negative correlation between the soil strength parameters ϕ and c. However, as discussed elsewhere [26], when the correlation (between c and ϕ) is assumed to equal zero the average bearing capacity is lower than any other average bearing capacity when correlation is assumed to be negative. On the other hand the standard deviation of bearing capacity under assumption of zero correlation is greater than any other bearing capacity standard deviation obtained under assumption of negative correlation.

Then, the random field of the lognormal distribution is obtained using the following equation:

$$c(\mathbf{x}) = \exp\left\{\mu_{\ln c} + \sigma_{\ln c} G_{\ln c}(\mathbf{x})\right\} \tag{12}$$

In the case of the internal friction angle, the standard Gaussian field, $G_\phi(\mathbf{x})$, is generated with a correlation structure equal to that of the cohesion field. After generating the random field ($G_\phi(\mathbf{x})$), the transformation to the bounded distribution field is obtained using

$$\phi(\mathbf{x}) = \phi_{\min} + \frac{1}{2}(\phi_{\max} - \phi_{\min})\left\{1 + \tanh\left(\frac{sG_\phi(\mathbf{x})}{2\pi}\right)\right\} \tag{13}$$

As previously mentioned, the computational core of the RFEM is the FEM. The bearing capacity of the soil was estimated using the FEM with an elastic perfectly plastic model and the Mohr–Coulomb failure criterion [28]. The random fields were adjusted to account for element size in the finite element mesh using the method of local averaging described by Fenton and Vanmarcke [10]. As a result, the mean value of the random field within a single element remained constant; the standard deviation changed and was averaged using the variance reduction function as follows:

$$\gamma^{\text{var}} = \frac{4}{(\alpha\theta_x)^2(\alpha\theta_y)^2}\int_0^{\alpha\theta}\int_0^{\alpha\theta}(\alpha\theta_x - \tau_x)(\alpha\theta_y - \tau_y) \times \exp\left(-\sqrt{\left(\frac{2\tau_x}{\theta_x}\right)^2 + \left(\frac{2\tau_y}{\theta_y}\right)^2}\right)d\tau_x d\tau_y \tag{14}$$

It is possible to determine the mean value and standard deviation of the bearing capacity by generating repeatedly different realisations of both random fields and carrying out a bearing capacity

estimation each time. However, the number of realisations in the simulation process must be selected to obtain stable bearing capacity statistics. As a result of several realisations for different initial pseudo-random numbers (seed), a stable mean value (with the probability of deviation less than 5%) was achieved using 300 realisations. The speed of the convergence is presented in Fig. 3.

3. Numerical analyses

The computer code that performs calculations using the deterministic FEM was calibrated so that the obtained results yielded similar values as the bearing capacity estimates from the analytical method (q_f), i.e., according to Eq. (1). The values of q_f have been calculated using N_γ, given by Eq. (15):

$$N_\gamma = 2\left[\exp(\pi \tan\phi\prime)\tan^2\left(\frac{\pi}{4}+\frac{\phi\prime}{2}\right)-1\right]\tan\phi\prime \tag{15}$$

Table 3 presents the results obtained for the situation shown in Fig. 3 with the soil parameters equal to the mean values in Table 2. The values of q_f were compared to the finite element computations (q_{FEM}) for the mean strength soil parameters. The FEM computations were performed for the mesh shown in Fig. 1, under the assumption the width of the foundation $B = 1$ m. The values of q_{FEM} are similar in each of these cases.

3.1. Isotropic case

The random soil resistance that was estimated under the assumption that the random fields of the strength parameters (cohesion and internal friction angle) are isotropic ($\theta_x = \theta_y = \theta$) was analysed. Fig. 4 presents the expected value of the bearing capacity as a function of the fluctuation scale (θ) standardised by the width of the foundation (B). Compared to the values given in Table 3, the results in Fig. 4 suggest that the expected value is lower than the deterministic value (q_{ult}). Within the range of the scales of fluctuation considered, the curves for all four cases have almost the same character (they are almost "parallel").

Local minima of the mean value with scales of fluctuations similar to the foundation width are observed in the various curves; this result is consistent with the observations of Griffiths and Fenton [15].

Fig. 5 shows the standard deviation of the random resistance. As with the mean value, the graph shows the dependence of the standard deviation on the normalised fluctuation scale. There is nearly a fourfold increase in the standard deviation of the resistance across the range of the analysed scales of fluctuations. The maximum increase is for the case of an embedded footing placed on a self-weight soil.

Considering the assessment of the random variability of the bearing capacity, the behaviour of the bearing capacity coefficient of variation (COVq_f), which is defined as the ratio of the standard deviation to the mean value of bearing capacity, can be calculated as

$$\mathrm{COV}q_f = \frac{\sigma_{q_f}}{\mu_{q_f}} \tag{16}$$

The dependence of the coefficient of variation on the fluctuation scale normalised by the width of a foundation is presented in Fig. 6.

The coefficient of variation had an increasing trend in all cases. The largest variation was observed in the case of the surface foundation placed on a weightless cohesive soil [1], which increased by nearly fivefold over the range of scales of fluctuations considered. Considering the weight of the soil [2], the change of COVq_f is minimal. The coefficient of variation behaves differently for the case of the embedded footing. The reduction of the variation of resistance due to the embedment of the foundation (the two lines at the bottom of the Fig. 6) can be seen. With the increase of the scale of fluctuation, the damping increases to nearly 20% when $\theta/B = 2$.

Table 3
Deterministic values for the mean parameters.

		q_f (kPa)	q_{FEM} (kPa)
[1]	Weightless cohesive soil, not embedded	538.50	528.49
[2]	Self-weight cohesive soil, not embedded	575.84	572.78
[3]	Weightless cohesive soil, embedded	660.09	647.99
[4]	Self-weight cohesive soil, embedded	697.43	694.88

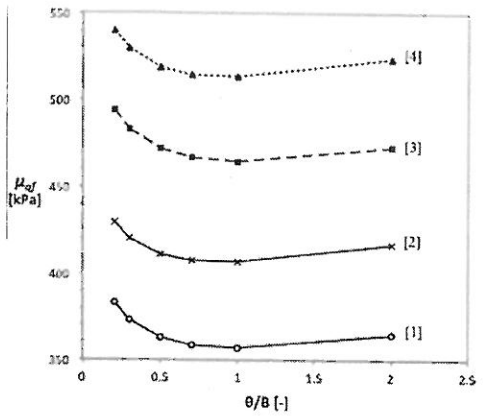

Fig. 4. Isotropic mean value for different computational cases: [1] surface foundation on a weightless soil, [2] surface foundation on a self-weight soil, [3] embedded footing on a weightless soil, and [4] embedded footing on a self-weight soil.

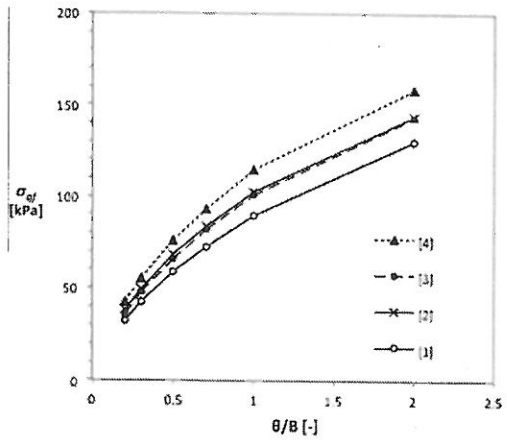

Fig. 5. Standard deviation of the bearing capacity for the isotropic task: [1] shallow foundation on a weightless soil, [2] shallow foundation on a self-weight soil, [3] embedded footing on weightless soil, and [4] embedded footing on a self-weight soil.

3.2. Anisotropic case

Soil properties are often more variable in the vertical direction than in the horizontal direction due to the sedimentary depositional processes. This phenomenon has been considered by Cherubini [7], who noted that the horizontal scale of fluctuation may be at least ten times the vertical scale. Therefore, an extended algorithm was used to analyse the impact of the anisotropic nature of random fields on the bearing capacity of soil. Only the vertical

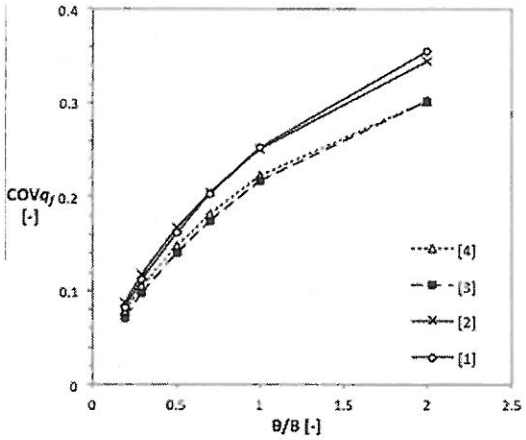

Fig. 6. Bearing capacity coefficient of the variation of soil for the isotropic task: [1] shallow foundation on a weightless soil, [2] shallow foundation on a self-weight soil, [3] embedded footing on a weightless soil, and [4] embedded footing on a self-weight soil.

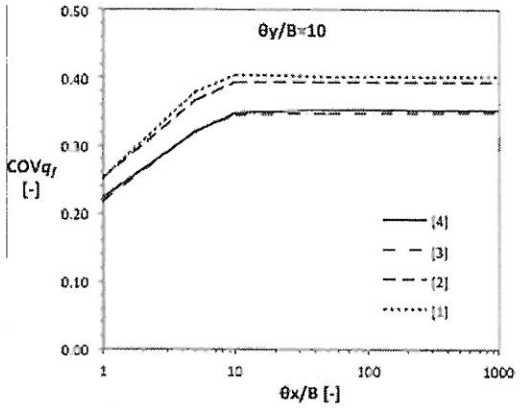

Fig. 8. Coefficient of variation and limit bearing capacity of resistance for four cases: [1] shallow foundation on a weightless soil, [2] shallow foundation on a self-weight soil, [3] embedded footing in a weightless soil, and [4] embedded footing in a self-weight soil.

scales were statistically determined by Cafaro et al. [5], as shown in Table 1; thus, in the present work, the horizontal scales in the range of 0.2–50 m were included in the parametric studies.

Fig. 7(a) shows the 3D surface of the average bearing capacity for the case of a footing embedded in self-weight soil. Fig. 7(b) shows the cross section of the surface for different θ_x/B values. Other cases provided a similar trend and are not shown here.

The cross-sections indicate the local minima for the horizontal scale of fluctuation, which occurs close to the width of the adopted foundation ($\theta_x/B = 1$). The mean value increases with an increase in the horizontal scale. The trend of the bearing capacity coefficient of variation (Fig. 8) levels out as θ_x/B increases. The coefficient of variation decreases in the case of an embedded footing but differs only slightly when including a self-weight soil. These observations are analogous to those observed in the isotropic case (Fig. 6).

A summary of the mean value for the anisotropic and isotropic cases (Fig. 9) indicates that the bearing capacity increases for values of horizontal scale of fluctuations that are larger than the width of the foundation. This increase is significantly smaller in the anisotropic case. The high values of the vertical scale (θ_y) are not likely in natural soils. Thus, the isotropic case may overestimate the

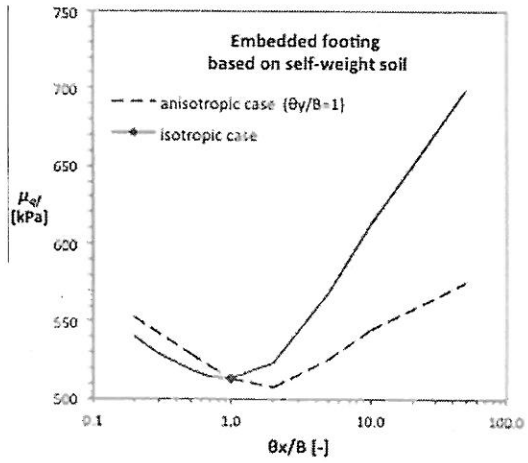

Fig. 9. Comparison of the mean value for the isotropic and anisotropic cases.

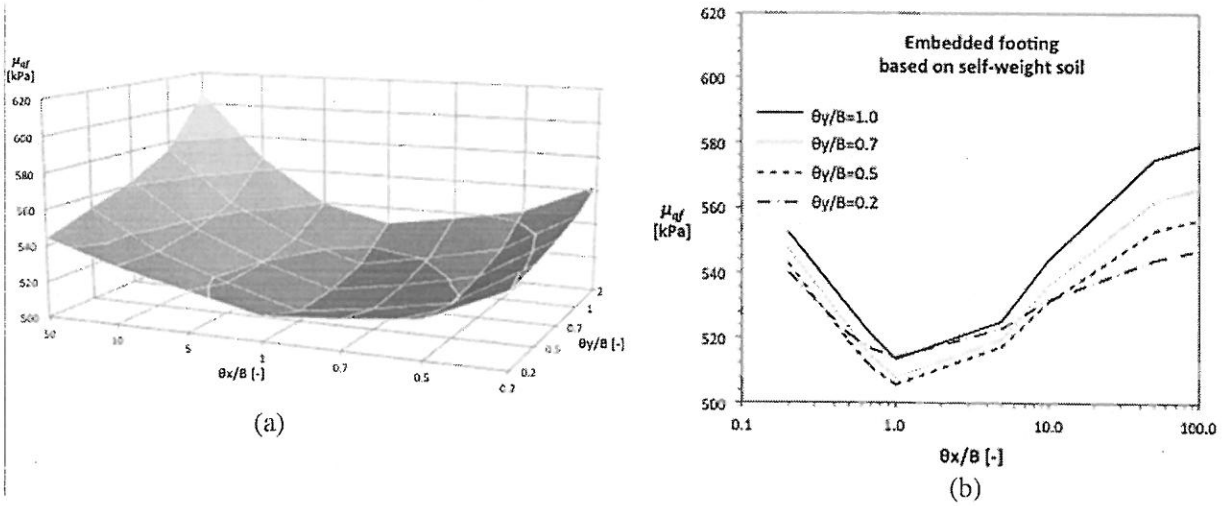

Fig. 7. Mean value of the bearing capacity for the anisotropic case: (a) the 3D surface; (b) the cross section of the surface for different θ_x/B values.

mean value of the bearing capacity (unconservative). In the anisotropic case, the vertical fluctuation scale was held constant at $\theta_y/B = 1$.

Analysing the coefficient of variation (Fig. 10), the anisotropic case yields a larger value for the coefficient of variation compared with the equivalent isotropic case. Thus, the isotropic case may underestimate the coefficient of variation of the bearing capacity, which can lead to unsafe values of reliability measures.

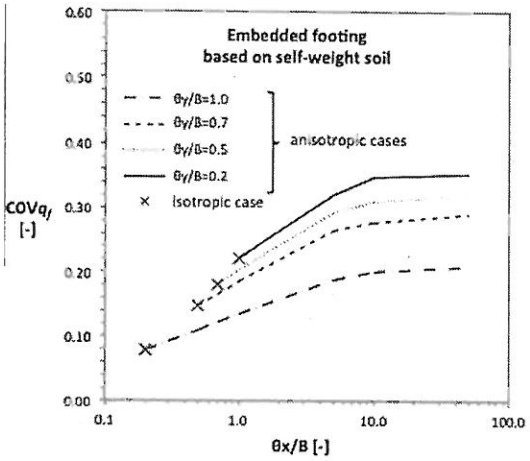

Fig. 10. Comparison of the bearing capacity coefficient of variation for the isotropic and anisotropic cases.

Table 4
Statistical values of the limit bearing capacity (anisotropic model, embedded footing, self-weight soil, $B = 1$ m, $\theta_x = 30$ m and $\theta_y = 0.7$ m).

Median	513 kPa
Arithmetic mean	520.7 kPa
Geometric mean	509.5 kPa
Variance	11689 $(kPa)^2$
Stand. deviation	108.1 kPa
Coef. of variation	0.2076 (–)
Third moment	5.31E+05 $(kPa)^3$
Stand. skewness	0.4204 (–)
Fourth moment	4.43E + 08 $(kPa)^4$
Stand. kurtosis	3.243 (–)

3.3. Probability distributions of a random soil bearing capacity

Values obtained as a result of the numerical analysis (RFEM) allowed for the estimation of the probability distribution of the bearing capacity. Here, the case of a footing embedded in a self-weight soil is analysed. Simulations were performed using 2000 realisations permitted the determination of stable values of high-order statistical moments. The case considered was for $B = 1$ m, $\theta_x = 30$ m and $\theta_y = 0.7$ m. Statistical parameters for the sample are summarised in Table 4.

A histogram was plotted from the 2000 realisations to determine the "best-fit" probability density function for the bearing capacity. As shown in Figs. 11 and 12, a lognormal fit was found to be a good model for the computed bearing capacity values.

In addition to the graphical goodness of fit, statistical tests were performed for the studied sample; these tests provided no basis to reject the lognormal distribution hypothesis. The results are presented in Table 5.

3.4. Application to reliability tasks

This manuscript presents only one of the cases of estimating the probability distribution (an anisotropic model, embedded footing, and self-weight soil). The same analysis was carried out for all of the studied computational cases (see Table 3). In all cases, lognormal fits were acceptable. The results were clear and are thus not included in this paper.

Results from the RFEM analysis of the bearing capacity of a shallow foundation enable the use of probability theory to analyse the reliability of a foundation. The estimated and tested probability distribution can be used to determine the probability of failure (p_f) or the reliability index (β).

$$p_f = P\{q_f \leqslant q_d\} = \Phi(-\beta) \tag{17}$$

where q_f is the random bearing capacity of the soil, which was obtained from analysis using the RFEM method, q_d is the design value of the bearing capacity, and Φ is the cumulative distribution function of the standard normal. Failure is defined as occurring when the bearing capacity is smaller than the design value.

Taking the logarithms of both sides of the inequality in the parentheses of Eq. (17) yielded the following:

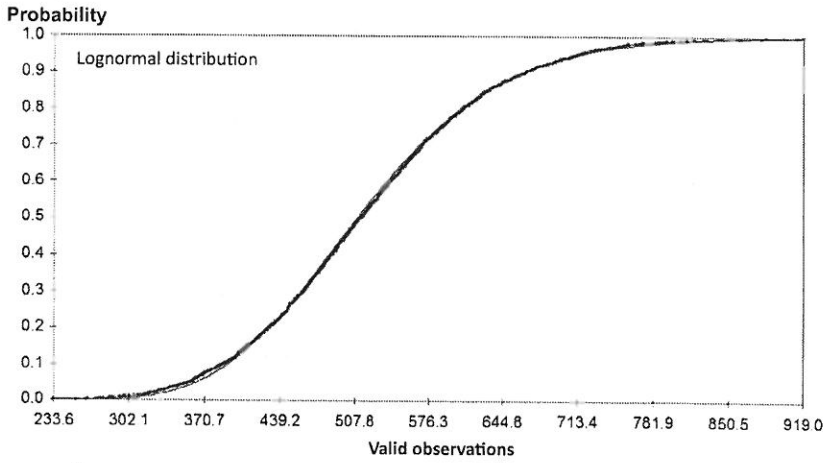

Fig. 11. Comparison of the cumulative distribution function from the RFEM with the theoretical distribution function for a lognormal distribution ($B = 1$ m, $\theta_x = 30$ m and $\theta_y = 0.7$ m).

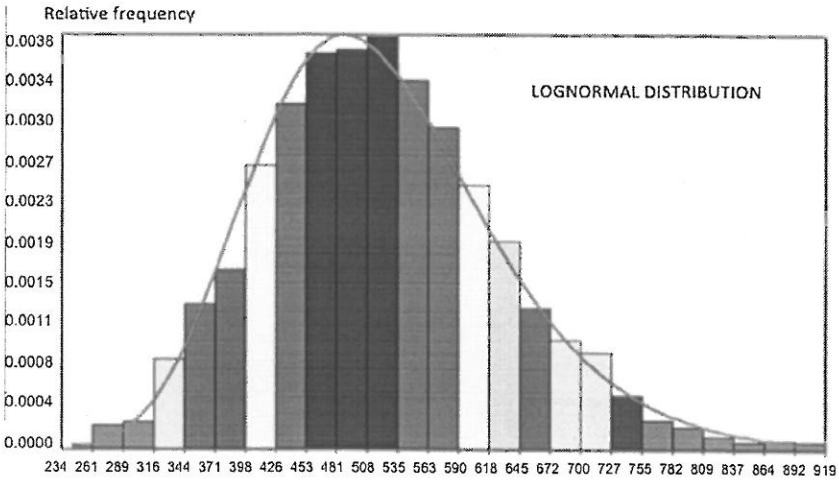

Fig. 12. Comparison of the histogram from the RFEM with the theoretical density function for a lognormal distribution (B = 1 m, θ_x = 30 m and θ_y = 0.7 m).

Table 5
Parameter estimation results obtained from the statistical tests of compliance (anisotropic model, embedded footing, and self-weight soil).

	Parameter estimation	
Selected estimation method	Method of moments	Least square method
Selected stochastic model	Lognormal	
Parameter 1 – $\mu_{\ln x}$	6.234	6.234
Parameter 2 – $\sigma_{\ln x}$	0.2055	0.2107
Testing		
Selected testing method	Kolmogorov–Smirnov test	
Significance level	0.4768	0.4842
Critical significance level	0.05	0.05
	The hypothesis should not be rejected	
Selected testing method	Chi-square distribution test	
Number of classes used in test	44	44
Significance level	0.3382	0.3728
Critical significance level	0.05	0.05
	The hypothesis should not be rejected	

$$p_f = P\{\ln q_f \le \ln q_d\} = P\left\{\frac{\ln q_f - \mu_{\ln q_f}}{\sigma_{\ln q_f}} \le \frac{\ln q_d - \mu_{\ln q_f}}{\sigma_{\ln q_f}}\right\} = \Phi\left(\frac{\ln q_d - \mu_{\ln q_f}}{\sigma_{\ln q_f}}\right) \tag{18}$$

$$\frac{\ln q_d - \mu_{\ln q_f}}{\sigma_{\ln q_f}} = -\beta \tag{19}$$

where $\mu_{\ln q_f}$ is the mean value of the underlying normal distribution in relation to the lognormal distribution of bearing capacity, q_f (9), and $\sigma_{\ln q_f}$ is the standard deviation of the underlying normal distribution (10). From Eq. (19), the design value of the bearing capacity can be determined as

$$\ln q_d = \mu_{\ln q_f} - \beta\sigma_{\ln q_f}$$
$$q_d = \exp\left\{\mu_{\ln q_f} - \beta\sigma_{\ln q_f}\right\} \tag{20}$$

Eq. (20) allows for the determination of the design value of the bearing capacity. The factor of safety can be defined as

$$\mathrm{FS} = \frac{\mu_{q_f}}{q_d} \tag{21}$$

where μ_{qf} is the expected value of the bearing capacity resulting from the RFEM computations.

Figs. 13 and 14 present the dependence of the design value of bearing capacity and the factor of safety (defined by Eq. (21) for the reliability index β), respectively. In these figures, the vertical scale of fluctuation was fixed at θ_y/B = 1, and several different values of the horizontal scale of θ_x/B were considered.

Fig. 13 illustrates that the design value of the bearing capacity decreases as the index β is increased. However, the value of the factor of safety increases (Fig. 14). Individual values stabilise with an increase in the horizontal scale of fluctuation of θ_x/B. The result is evident when the scale of fluctuation is larger than 5.

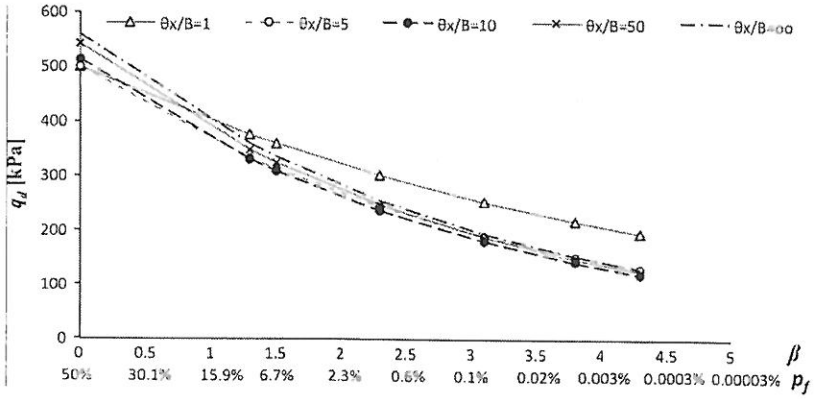

Fig. 13. Design value of the bearing capacity for different β and θ_x/B values (θ_y/B = 1).

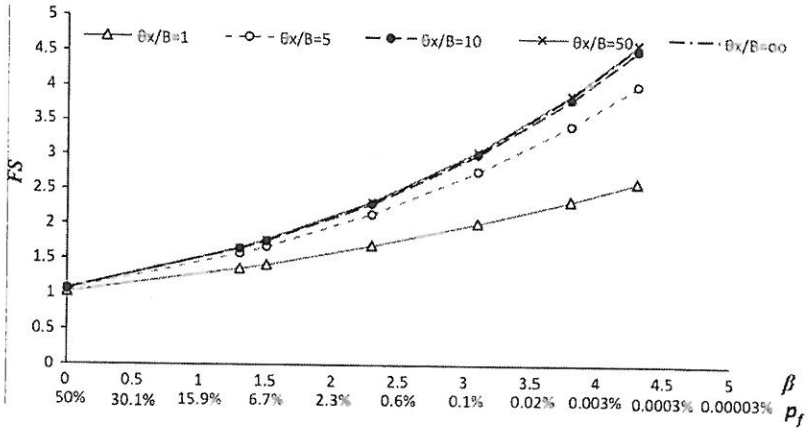

Fig. 14. Factor of safety for the resistance depending on the β indicator for $\theta_y/B = 1$ and different θ_x/B values.

The presented design value can be the starting point for the calibration of safety factors with the use of any method, such as the global factor or the method of partial coefficients for the entire resistance, which is promoted by European standards [17]. Fig. 14 provides examples of the calibration of the partial safety factor of resistance.

4. Concluding remarks

This paper describes an extension to existing work to include the impact of embedment and soil self-weight on the bearing capacity of a footing on random soil. The existing RFEM code [11] was modified and extended to capture the above mentioned factors.

Two main conclusions can be summarised as follows:

(1) The coefficient of variation of the bearing capacity is reduced by the influence of embedment but is not reduced by the inclusion of self-weight.
(2) Including anisotropy decreases the mean and increases the variance of the bearing capacity compared to the isotropic case. Both of these factors suggest that the isotropic case may lead to unsafe estimates of reliability.

For the cases considered, a lognormal distribution for the bearing capacity was observed from the RFEM results. The lognormal distribution may be dominated by the cohesion field, which also has a lognormal distribution and is linearly related to the bearing capacity. Provided that the coefficient of variation of the cohesion, c, is significantly greater than the coefficient of variation of the friction angle, ϕ, the distribution of the bearing capacity, q_f, may follow that of the cohesion distribution.

Calibration of the factor of safety showed that the design value of the bearing capacity and the design values of safety factors stabilise for a horizontal scale greater than or equal to $\theta_x/B = 10$.

Future studies may also include further modifications to the RFEM code such as including more sophisticated soil models, pore pressures and consideration of 3D.

Acknowledgement

This article, as a research project, was supported by the Polish National Science Center (NCN) under the Grant No.: N N506 158338, funds for science in years 2010–2013.

References

[1] Ahmed A, Soubra A. Probabilistic analysis of strip footings resting on a spatially random soil using subset simulation approach. Georisk 2012;6(3):188–201.
[2] Al-Bittar T, Soubra A. Bearing capacity of strip footings on spatially random soils using sparse polynomial chaos expansion. Int. J Numer Anal Meth Geomech 2012;37:2039–60.
[3] Alonso E, Krizek RJ. Stochastic formulation of soil properties. In: Proceedings of the 2nd international conference on applications of statistics and probability in soil and structural engineering, vol. II. Aachen; 1975. p. 9–32.
[4] Cafaro F, Cherubini C, Cotecchia F. Use of the scale of fluctuation to describe the geotechnical variability of an Italian clay. In: Melchers, Stewart, editors. Proceeding of the 8th international conference on applications of statistics and probability in civil engineering, Rotterdam; 2000: p. 481–6.
[5] Cafaro F, Cherubini C. Large sample spacing in evaluation of vertical strength variability of clayey soil. J Geotech Geoenviron Eng 2002;128(7):558–68.
[6] Cassidy MJ, Uzielli M, Tian Y. Probabilistic combined loading failure envelopes of a strip footing. Comput Geotech 2013;49:191–205.
[7] Cherubini C. Data and consideration on the variability of geotechnical properties of soils. In: Proceedings of the ESREL Conference, Lisboan; 1997: p 1538–91.
[8] Cherubini C. Probabilistic approach to the design of anchored sheet pile walls. Comput Geotech 2000;26(3–4):309–30.
[9] Cherubini C, Vessia G, Pula W. Statistical soil characterization of Italian sites for reliability analysis. In: Tan W, Phoon KK, Hight, Lerouell, editors. Characterization and Engineering properties of natural soil, Singapore, Taiwan; 2007: p. 2681–706.
[10] Fenton GA, Vanmarcke E. Simulation of random fields via local average subdivision. ASCE J Geotech Eng 1990;116(8):1733–49.
[11] Fenton GA, Griffiths DV. Bearing capacity prediction of spatially random c-φ soils. Can Geotech J 2003;40(1):54–65.
[12] Fenton GA, Griffiths DV. Reply to discussion by R. Popescu on, Bearing capacity prediction of spatially random c – φ soils. Can Geotech J 2004;41:368–9.
[13] Fenton GA, Griffiths DV. Risk assessment in geotechnical engineering. Hoboken, N.J: John Wiley & Sons; 2008.
[14] Fenton GA, Zhang XY, Griffiths DV. Reliability of shallow foundations designed against bearing failure using LRFD. Georisk: Assess Manage Risk Eng Syst Geohazard 2007;1(4):202–15.
[15] Griffiths DV, Fenton GA. Bearing capacity of spatially random soil: the undrained clay Prandtl problem revisited. Geotechnique 2001;51(8):731.
[16] Griffiths DV, Fenton GA. Seepage beneath water retaining structures founded on spatially random soil. Geotechnique 1993;43(6):577–87.
[17] ISO:2394. General principles on reliability for structures; 1998.
[18] Kasama K, Whittle AJ. Bearing capacity of spatially random cohesive soil using numerical limit analyses. J Geotech Geoenviron Eng 2011:989–96.
[19] Krige DG. A statistical approach to some basic mine valuation problems on the Witwatersrand. J Chem Metall Min Soc S Afr 1951;52(6):119–39.
[20] Krige DG. Statistical applications in mine valuation. J Inst Mine Surv S Afr 1962;12(2):S45–84 [12(3):95–136].
[21] Lumb P. The variability of natural soils. Can Geotech J 1966;3(2):74–97.
[22] Lumb P. Safety factors and the probability distributions of soil strength. Can Geotech J 1970;7(3):225–42.
[23] Lumb P. Spatial variability of soil properties. In: Proceedings of the 2nd international conference on applications of statistics and probability in soil and structural engineering (ICASP), vol. II. Aachen; 1975. p. 397–422.
[24] Page ES. Continuous inspection scheme. Biometrika 1954;41(1/2):100–15.
[25] Prandtl L. [Uber die Harte plastischer Korper]. Mathematisch-physikalische Klasse aus dem Jahre 1920:74–85 [Germany].

[26] Pieczynska J, Puła W, Griffiths DV, Fenton GA. Probabilistic characteristics of strip footing bearing capacity evaluated by random finite element method. In: Proceedings of the 11th international conference on applications of statistics and probability in soil and structural engineering (ICASP), Zurich; 2011. [Paper No. 10321, CD-ROM].
[27] Rahman MM, Nguyen HBK. Applications of Random Finite Element Method in Bearing Capacity Problems. In: Proceedings of the 6th international conference on advanced engineering computing and applications in sciences (ADVCOMP 2012), Barcelona; 2012.
[28] Smith IM, Griffiths DV. Programming the finite element method. 4th ed. New York: J. Wiley & Sons; 2004.
[29] Schultze E. Frequency distributions and correlations of soil properties. In: Lumb P, editor. Proceedings of the 1st International Conference on Applications of Statistics and Probability in Soil and Structural Engineering (ICASP), Hong-Kong, University Press, Hong-Kong; 1972. p. 372–87.
[30] Terzaghi K. Theoretical soil mechanics. New York: John Wiley & Sons; 1943.
[31] Vanmarcke EH. Probabilistic modeling of soil profiles. J Geotech Eng Div, ASCE 1977;103(GT11):1227–46.
[32] Vanmarcke EH. Reliability of earth slopes. J Geotech Eng Div, ASCE 1977;103(GT11):1247–65.
[33] Vanmarcke EH. Random fields-analysis and synthesis. Cambridge: MIT Press; 1983.
[34] Zubrzycki S. [On estimating gangue parameters]. Zastosowania Matematyki 1958;3 105–153 [Poland].